High-order harmonic generation experiments with IR laser pulses

D. Comtois*[a], H.-C. Bandulet*[a], E. Bisson[a], A. Borowiec[b], H. Pépin[a], P. B. Corkum[b], J.-C. Kieffer[a], D. M. Villeneuve[b]
[a]INRS-Énergie, Matériaux et Télécommunications, 1650 boul. Lionel-Boulet, Varennes, QC, Canada J3X 1S2;
[b]National Research Council, 100 Sussex Drive, Ottawa, ON, Canada K1A 0R6

ABSTRACT

We report on the first experiments of high-order harmonic generation done with the 100 Hz high-energy optical parametric amplifier (OPA) of the Advanced Laser Light Source. Using krypton and argon as targets, we show that the OPA's signal beam – with a wavelength range from 1200 nm to 1600 nm, 1.3 mJ to 0.8 mJ of pulse energy and 100 fs pulse duration – can generate fully tunable XUV radiation down to a wavelength of 15 nm. We have also started to investigate the use of the OPA pulses for molecular imaging. Inducing molecular alignment with 800 nm, 70 fs pulses, we have measured the high harmonics spectra generated with 1300 nm pulses from nitrogen molecules oriented at various angles with respect to the ionizing field, in order to study for the first time the technique of molecular orbital tomography with a laser wavelength different than 800 nm.

1. INTRODUCTION

High harmonic generation (HHG) via the interaction of an intense laser pulse with a gas has been widely studied in the past with fixed-wavelength laser systems, such as Ti:Sapphire (λ = 800 nm) and neodymium-doped (λ = 1 μm) lasers. The few studies to have been so far realized using longer wavelength drivers from optical parametric amplifiers (OPA) were limited to an on-target energy of 150 μJ [1-3]. However, the development of high energy OPAs and optical parametric chirped pulse amplifiers (OPCPAs) is now making the use of infrared (IR) pulses more interesting for HHG experiments. The 100 Hz repetition rate OPA available at the Advanced Laser Light Source (in Varennes, Canada) provides 100 fs pulses with an energy around 1 mJ in the 1.2 μm to 1.6 μm range; an energy level for which HHG becomes practical.

HHG has many potential applications as a source of coherent XUV radiation, like ultrafast spectroscopy [4], water-window holography of living cells [5-7] or x-ray laser seeding [8]. With the usual fixed-wavelength laser systems, however, the XUV radiation from HHG is limited to narrow spectral ranges. This limitation is removed with the use of an adjustable OPA. The IR pulses provided by an OPA also have the advantage of allowing the production of HHG photons of higher energy [2,9]. This can be understood within the framework of the three-step model of HHG [10]: When an atom or molecule is submitted to an intense laser pulse, an electron wave packet 1) is released in the continuum through tunneling ionization, 2) driven away and back to the parent ion by the oscillating laser field and 3) recollides with it and recombines back into the atom or molecule's ground state wave function, leading to the emission of an XUV photon. The highest photon energy emitted in the HHG process (cutoff energy) corresponds to the maximum recollision energy of the electron wave packet and is equal to $3.2U_P + I_P$, where U_p is the electron's ponderomotive energy in the laser field and I_p is the atom or molecule's ionization potential. Thus, since U_p is proportional to the square of the driving field's wavelength, the same is closely true for the HHG cutoff energy.

In recent years, high harmonic generation has also emerged as a powerful tool for probing molecular structure and observing molecular dynamics on the femtosecond, and even attosecond, timescales. In the HHG process, the recombining electron wave packet interferes with the ground state wave function of the target molecule. The different frequency components of the wave packet undergo different degrees of interference, leading to modulations in the HHG spectra from aligned molecules [11-14] that provide information about their structure. It was also found that, by

* these authors contributed equally to this work: comtois@emt.inrs.ca, bandulet@emt.inrs.ca

Ultrafast X-Ray Sources and Detectors, edited by Zenghu Chang, George A. Kyrala, Jean-Claude Kieffer,
Proc. of SPIE Vol. 6703, 67030E, (2007) · 0277-786X/07/$18 · doi: 10.1117/12.735256

measuring HHG spectra for all orientations of the nitrogen molecule with respect to the laser field, it is possible to take advantage of these interference effects and use a tomography algorithm to make a complete reconstruction of its highest occupied molecular orbital (HOMO) [15-16]. Demonstrated for the case of static molecules, this technique opens the door for the direct observation of changes in orbital shapes as molecular bonds are broken and created, which is the basis of chemical processes. For such molecular imaging techniques, the recolliding wave packet's energy is a crucial parameter, as its de Broglie wavelength has to be short enough for interference with the ground state wave function to occur. The ability to increase the recollision energy by using longer driver wavelengths would therefore increase the range of molecules that could be probed with HHG, since high enough recollision energies could be obtained for molecules with lower ionization potential. For molecules that can already be probed with 800 nm light, an increase of the recollision energy results in sampling the orbital with higher frequencies, which improves the imaging resolution.

It was shown that HHG can also be used to probe the motion of protons in molecules with attosecond resolution [17], by measuring HHG spectra for special molecule pairs: one molecule containing protons and the other one for which they have been substituted for deuterons (like H_2/D_2 and CH_4/CD_4). Different isotopes move at different velocities and hence do not yield the same harmonic intensity for a given recollision time. Since the recolliding electron wave packet is chirped (the recollision energy varies with time), the ratio between the spectra from an isotope pair is a time map of proton motion. A longer driver wavelength is very interesting for molecular dynamics measurements with this technique, since it increases the observation time window.

The use of high harmonics produced with femtosecond IR pulses as an XUV radiation source and for molecular imaging is investigated at the Advanced Laser Light Source. In this paper, we first introduce the laser source and experimental setup used for the HHG experiments. We then present some results of HHG spectra obtained by ionizing krypton and argon using pulses with a wavelength between 1200 nm and 1600 nm and demonstrate the adjustability of the XUV radiation produced. Finally, we show preliminary results of the first measurement of molecular orbital tomography done with 1.3 μm driving laser pulses. The measurement was performed on the nitrogen molecule (as in [15]), in order to demonstrate the use of the technique with longer laser wavelengths.

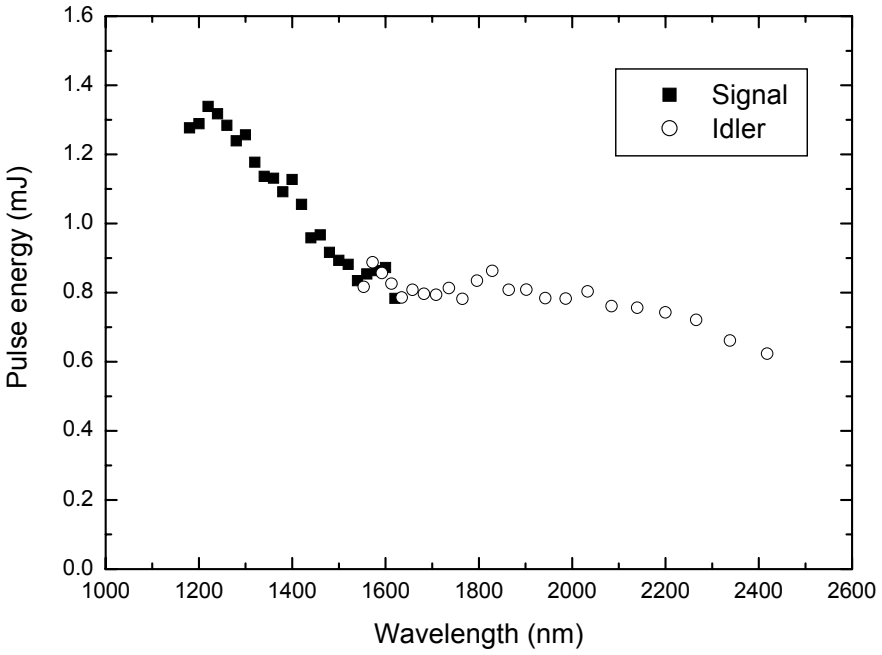

Fig. 1. Output pulse energy versus wavelength for signal and idler beams from ALLS's 100 Hz HE-TOPAS. Pulse duration is 100 fs.

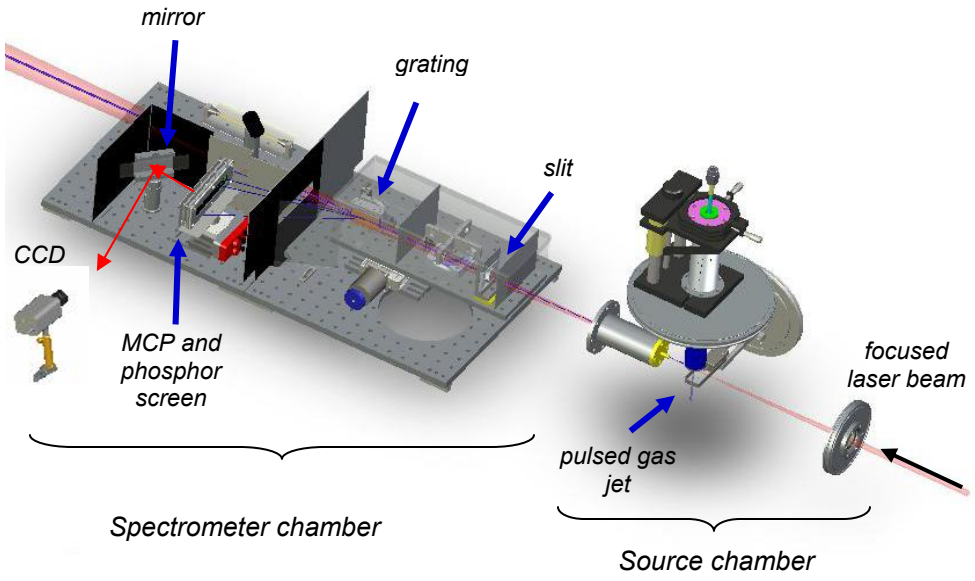

Fig. 2. The HHG vacuum chamber.

2. EXPERIMENTAL TOOLS

HHG experiments at the ALLS are performed with a 100-Hz repetition rate Ti:Sapphire laser system from Thales (λ = 800 nm). This laser is used to pump an HE-TOPAS (High-Energy Travelling-wave Optical Parametric Amplifier of Superfluorescence) system from Light Conversion, with 7 mJ, 70 fs long (negatively chirped) pulses. The signal and idler beams at the output of the HE-TOPAS have a diameter of 10 mm. Their wavelength can be continuously tuned from 1200 nm to 1600 nm for the signal beam and from 1600 nm to 2400 nm for the idler beam. The signal pulse energy varies between 1.3 mJ and 0.8 mJ, whereas the idler pulse energy is between 0.8 mJ and 0.6 mJ (see Fig. 1 for the energy tuning curve). The duration of the signal pulses is around 100 fs, measured with an autocorrelator.

The HHG vacuum chamber is made of two parts: the source and spectrometer chambers (Fig. 2). With a lens located before the source chamber entrance window, the HHG driver beam is focused in a gas jet expanding from a 200 µm diameter pinhole at the output of a pulsed valve mounted on an XYZ translation stage. The harmonics produced through the interaction of the driver beam with the gas jet pass through a 3 mm diameter hole between the source (pressure ~10^{-4} torr during gas jet operation) and spectrometer (pressure ~10^{-6} torr) chambers. Inside the spectrometer chamber, the harmonic radiation is filtered through a 100-µm alumina slit and spectrally dispersed by a 1200 l/mm Hitachi concave grating. The radiation is then imaged onto the surface of a chevron microchannel plate detector with phosphor screen. A 16-bit CCD camera is used to capture the spectra displayed on the phosphor screen through a window and via a plane mirror located in the chamber. The MCP detector plane is installed to catch harmonics spectral lines below a wavelength of 100 nm.

3. RESULTS

3.1 Tunable harmonics with an IR driver

Harmonics were generated in krypton (I_p = 14.0 eV) and argon (I_p = 15.8 eV), with a pulsed valve backing pressure of 4 bars, using the signal beam at various wavelengths. Typical spectra in each gas are shown in Fig. 3. The laser pulse

energy just before focusing was varied between ~1.1 mJ at 1300 nm and ~700 μJ at 1520 nm. As expected, the spectra show a smaller spacing between neighboring harmonic orders as the driver wavelength is increased, and the wavelength of a given order shifts to a lower value (see Fig. 3). For instance, one can directly see in Fig. 3 that the wavelength of the 17th harmonic generated at 1520 nm is longer than the wavelength of the 15th harmonic produced at 1200 nm. The adjustability of the driving field wavelength makes it possible to generate harmonics at any desired wavelength from about 200 nm down to the cutoff. The harmonics generated with the signal beam can then be used as a tunable coherent XUV radiation source.

The highest observable harmonic order in the krypton spectra of Fig. 3 decreases for a longer driver wavelength, and so does the overall harmonic yield, because of the decreasing energy of the signal pulses. The increase of the focal spot size with wavelength (area $\propto \lambda^2$) adds to this effect.

In these measurements, we have been able to observe up to the 59th harmonic at 1300 nm in krypton. According to the law giving the cutoff energy of harmonics emission ($I_p + 3.2U_p$), a cutoff at this position would mean a focal spot intensity of about 6×10^{13} W/cm^2. This number is well below the saturation intensity of Krypton of 1.5×10^{14} W/cm^2. However, using argon (I_p = 15.8 eV) with the 1300 nm beam, we could see up to the 85th harmonic, which means a focal spot intensity of at least 1×10^{14} W/cm^2 (while the saturation intensity of Argon is 2.5×10^{14} W/cm^2). We therefore believe that our spectrometer setup is currently not able to detect the full harmonic spectra generated in our IR wavelength range. By contrast, we have no problem measuring spectra up to the well known cutoff frequencies when we ionize krypton or argon directly with the 800 nm pulses from the Ti:Sapphire laser.

These observations could be explained by the much lower HHG conversion efficiency expected when the wavelength of the driving field is increased. A recent theoretical study [9] concludes that the harmonics yield scales as $\lambda^{-(5\text{-}6)}$ at constant intensity. Furthermore, these calculations show that the yield close to the cutoff is much lower for the long driver wavelengths than it is for 800 nm. Hence, a better detection system seems necessary to observe the full spectra produced at long wavelengths.

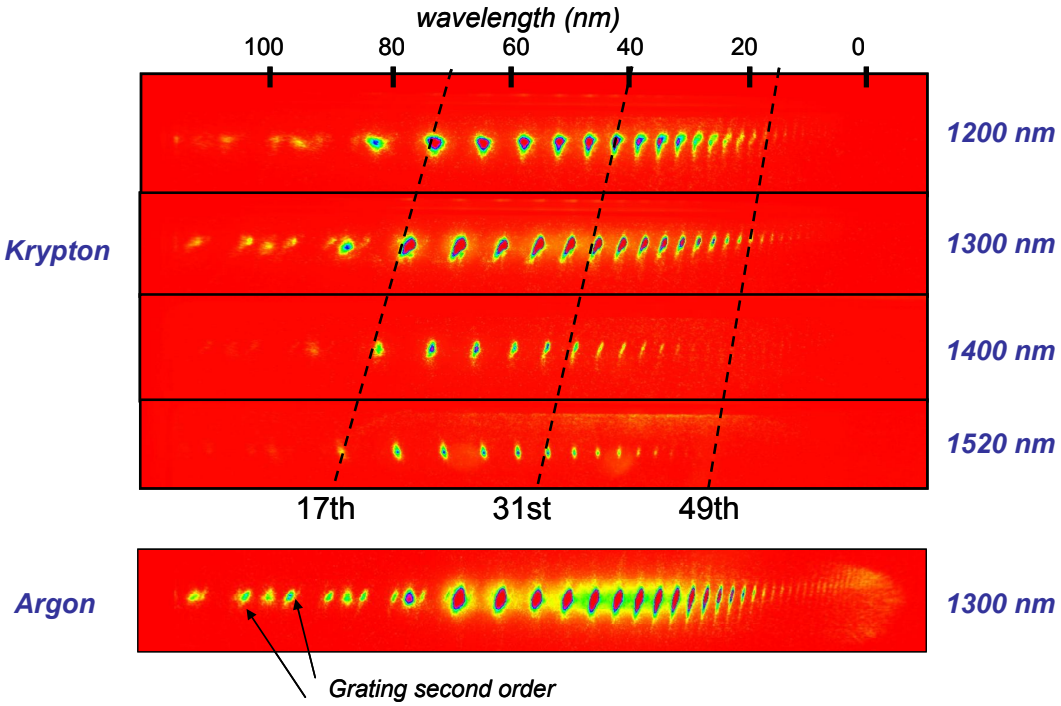

Fig. 3. High-order harmonic spectra generated in krypton and argon for various wavelengths of the signal beam (for different intensities), with an f = 300 mm focusing lens. Visible satelittes in the lower orders correspond to the second order peaks of the spectrometer grating.

3.2 Preliminary results: molecular orbital tomography of nitrogen at λ = 1.3 μm

In this section, we show the first set of harmonic spectra from laser-aligned nitrogen molecules using an OPA IR beam that was taken in order to develop the technique of molecular orbital tomography. Because it rendered the maximum output energy, we have chosen to work with a wavelength of 1300 nm to reproduce the measurement of molecular tomography of the nitrogen molecule's HOMO reported in [15], which was done using 800 nm beams only.

Molecular orbital tomography, as described in [15], is achieved by using two (pump and probe) femtosecond laser pulses. The pump pulse is focused in the gas jet with a laser intensity that is slightly below the ionization threshold of the molecule. This pulse polarizes the molecules and gives them a kick in angular momentum that leads to the creation of a rotational wave packet [18]. Shortly after passage of the laser pulse, the molecules are aligned around the pump laser field polarization axis. This alignment rapidly vanishes, but reoccurs periodically with a time period determined by the molecule's rotational time constant. The probe pulse is then sent at a time which coincides with a revival in the molecular alignment. The polarization of the pump pulse is rotated, and HHG spectra are recorded for a series of angles between the molecules and the ionizing laser field.

The spectral intensity of harmonics emission is given by the Fourier transform of the acceleration of the transition dipole moment from the ionized molecule's HOMO to the continuum electron's wavefunction [19]: $S(\omega) \propto \omega^4 |d(\omega)|^2$. The amplitude of the transition dipole moment itself in the spectral domain $d(\omega)$ can be detailed as:

$$d(\omega) = a[k(\omega)] \int \psi_g(\mathbf{r})(e\mathbf{r}) \exp[ik(\omega)x] d\mathbf{r} \tag{1}$$

We find in here the ground state wave function of the molecule of interest $\psi_g(\mathbf{r})$ and the spectral components of the electron wave packet ψ_c, which can be represented as a set of plane waves:

$$\psi_c = \int a[k(\omega)] \exp[ik(\omega)x] dk \tag{2}$$

where $a[k(\omega)]$ is the complex amplitude of the wave packet component with wavenumber $k(\omega)$ and x is the polarization axis of the ionizing laser field. Hence, the experimental data provide a measurement of the Fourier transform of the function $\mathbf{r}\psi_g(\mathbf{r})$ for different orientations of $\psi_g(\mathbf{r})$. By analyzing this measurement with mathematical algorithms developed for computer-assisted tomography, the molecular orbital $\psi_g(\mathbf{r})$ can be fully reconstructed, with both amplitude and phase (see [15] for more details). The only experimental unknown is the electron wave packet amplitude $a[k(\omega)]$. This problem is solved by calibrating it using an HHG spectrum taken with an atom having a similar ionization potential to that of the molecule of interest – and for which the electron wave packet is alike. In the case of nitrogen, the chosen companion atom is argon.

In our experiment, we used two output beams from the HE-TOPAS: the signal beam, tuned to a wavelength of 1300 nm, and the remaining part of the 800 nm pump beam after being used for optical parametric amplification. The former was probing the molecules through HHG and the latter (the pump) was producing molecular alignment. The optical layout of the experiment is shown in Fig. 4. The optical path length of the pump beam could be adjusted by two mirrors on a motorized translation stage. Its polarization could be rotated by a half-waveplate mounted on a motorized rotation stage. Just after this waveplate, the signal and depleted pump beams were combined on the same optical path by a hot mirror. Using two steering mirrors, the beams passed through an f = 300 mm lens and sent in the chamber. The angle of incidence of the beams on the hot mirror and the two following mirrors was close to zero degree, in order to be able to use any polarization of the pump beam. The energy of the signal beam was 1 mJ. It was focused slightly before the gas jet, with an intensity estimated about (1-2)×10^{14} W/cm^2. The pump beam was focused by the lens a few millimeters before the signal beam. Since the pump beam had a lot of energy (a few mJ), we used an iris diaphragm to limit its intensity to values below the threshold for observable harmonic generation (below 250 μJ). A reduction in its beam diameter also extended its Rayleigh range to facilitate the overlap with that of the signal beam. Another iris located just before the focusing lens was used to control the focusing conditions of the signal beam.

Prior to the spectral measurements, it was necessary to determine the experimental parameters for molecular alignment. This was realized by monitoring the HHG yield as a function of the time delay between the pump and the probe, as it is known that the HHG yield is higher for nitrogen molecules parallel to the ionizing field than for molecules perpendicular

to it [20]. Fig. 5 displays the variation of the yield of the 25th to the 39th harmonics with pump-probe delay around the first half-revival of the nitrogen rotational wave packet, in the conditions chosen for the experiment. Maximum HHG yield - and thus maximum alignment - is obtained for a pump-probe delay of 4 ps. The delay was fixed at this position for the tomography measurement.

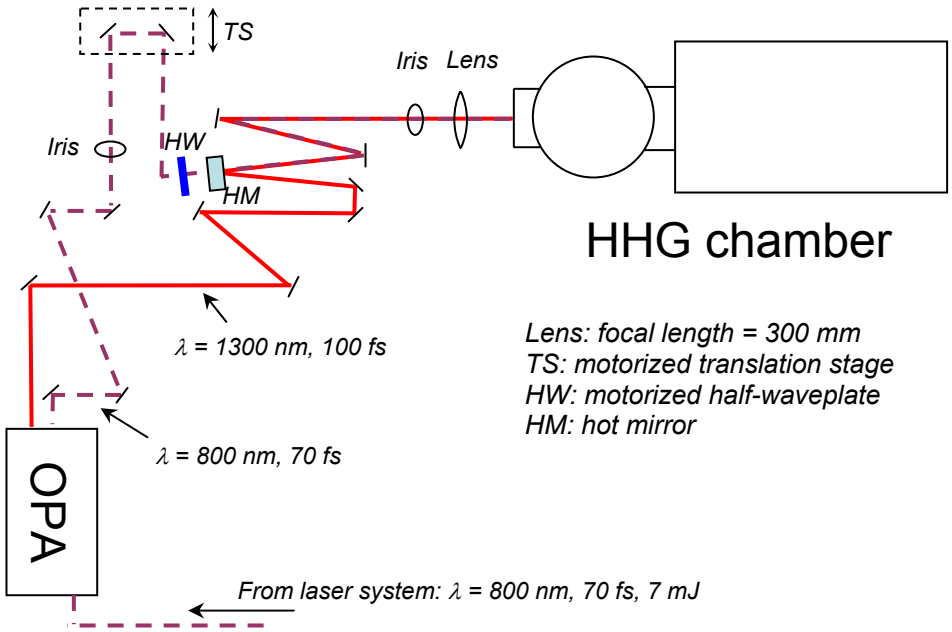

Fig. 4. Optical layout for molecular orbital tomography

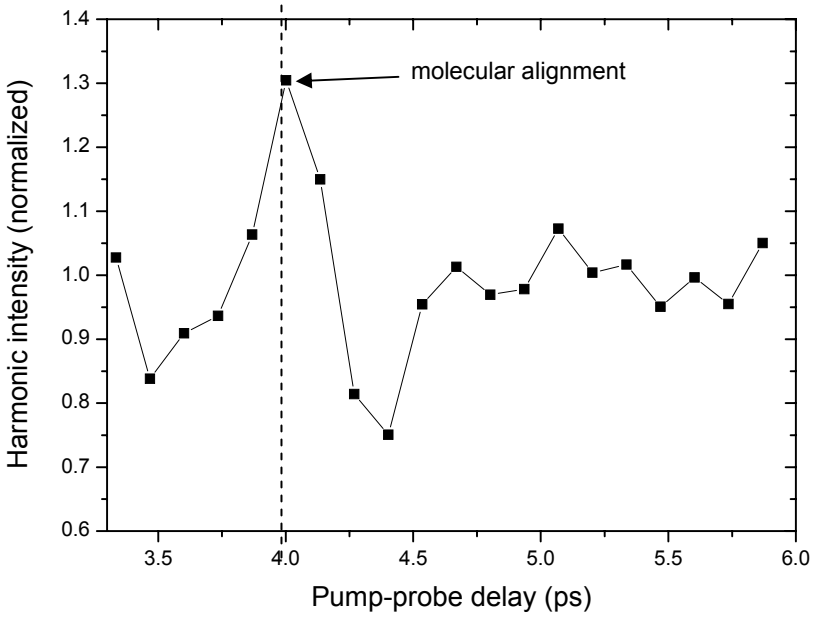

Fig. 5. Harmonic intensity versus delay between the pump (aligning) and the probe (HHG) pulses, integrated from the 25th order to the 39th order.

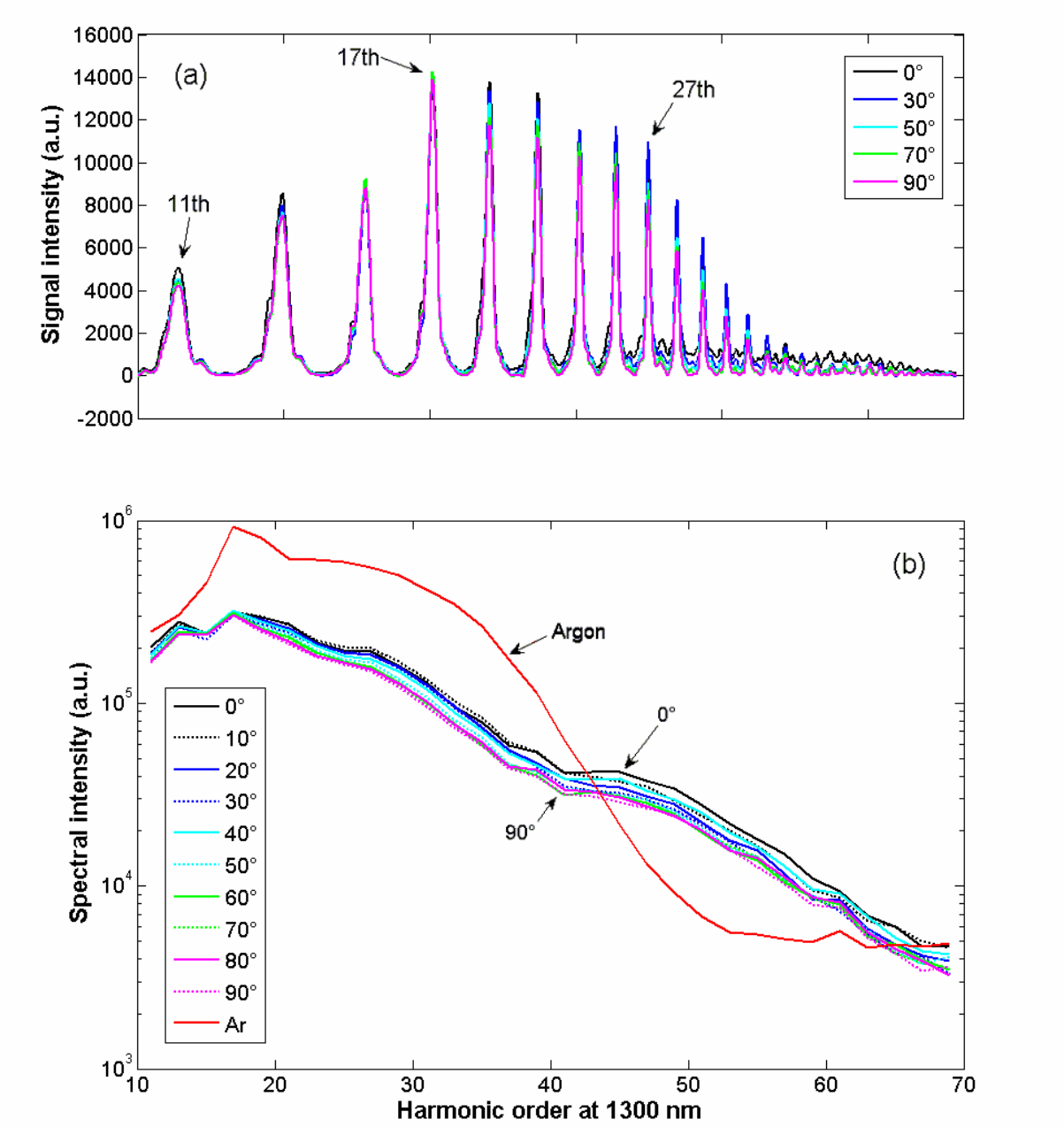

Fig. 6. High harmonic spectra produced in N_2 molecules by a 1300 nm laser field. The molecular alignment axis is varied every 10° between 0 and 90° relative to the polarization axis of the ionization laser field. For clarity, only some of the angles are plotted above. (a) Background-subtracted lineouts of the spectra (averaged spatially over the harmonic beam diameter). (b) Integrated harmonic signal as a function of harmonic order for different alignment angles. The high harmonic spectrum from argon (reference atom) is also shown. The spectra depend on both the alignment angle and shape of the ionized orbital.

The HHG spectra of nitrogen (pulsed valve backing pressure of 4 bars) were recorded with the angle of molecular alignment relative to the ionizing beam polarization axis being rotated every 10° between 0° and 90°. The spectra that were obtained for some selected angles are shown in Fig. 6(a). Each spectrum begins at the 11th harmonic and exhibits visible orders up to about the 83rd harmonic, even though beyond the 71st harmonic, the individual harmonics are too

close together to be distinguishable. Again, the highest visible harmonic order does not reach the expected theoretical cutoff for a 1300 nm wavelength driver, which is expected at around the 183rd harmonic. In fact, the 83rd harmonic of a 1300 nm wavelength field corresponds to about the 51st of an 800 nm field, which is roughly the cutoff order in nitrogen at this wavelength. As explained in the previous section, we believe that higher sensitivity is required to observe the higher orders with the wavelength used.

The measured spectra exhibit clear modulations with variation of the angle of molecular alignment in N_2. One can see on both Fig. 6(a) and 6(b) that the overall harmonic yield decreases as the molecular and laser polarization axes are closer to being orthogonal. This is especially true for orders above the 19th. On the other hand, from the 11th harmonic to the 17th harmonic, the yield does not vary much with molecular alignment, as one can see from Fig. 6(b) displaying the integrated spectral intensity as a function of the harmonic order. This behavior hasn't been observed by Itatani *et al*. as only harmonics above order 17 at 800 nm were analyzed [15], which is equivalent to the 27th order at 1300 nm. Also shown on Fig. 6(b) is the spectral intensity of the harmonic emission in argon — the reference atom — recorded in the same conditions as nitrogen. Besides it dependence on the molecular alignment angle (thus invariant for atoms), one can see that the spectrum also varies with the shape of the ionized orbital.

The spectral intensity measurements of Fig. 6(b) in argon and nitrogen should enable the reconstruction of the N_2 HOMO. This result will then be compared to the previous reconstruction using an 800 nm driver. This work is ongoing. In our next set of experiments, we should apply the tomography technique to probing molecules of low I_p, for which a long wavelength driver is required.

4. CONCLUSION

High-order harmonic generation has been tested using the 100-Hz repetition rate OPA beam line of the Advanced Laser Light Source. We have shown that the OPA's signal beam (wavelength tuned between 1200 nm and 1600 nm), can be used to generate harmonics in krypton and argon that make a coherent XUV source with a fully tunable wavelength down to 15 nm (85th harmonic of argon at 1300 nm). We have also demonstrated that the OPA can be used for molecular imaging experiments, by performing measurements of molecular orbital tomography of nitrogen with 1.3 μm pulses.

In the future, the experimental setup will have to be improved in order to observe the high harmonics cutoff extension expected from the use of longer driver wavelengths. This will make high harmonics generation with the OPA beam line even more interesting as an XUV source and will allow to improve the resolution of molecular imaging measurements by probing molecules with shorter de Broglie wavelength components of the recolliding electron wave packet. There are also plans to investigate HHG phenomena using the idler beam, which will require tighter beam focusing. Finally, the development of pulse compression techniques to generate few-cycle pulses in the IR will be useful for molecular dynamics experiments.

REFERENCES

1. M. Bellini, "Generation of widely tunable harmonic pulses in the UV and VUV from a NIR optical parametric amplifier", *Appl. Phys. B* 70, 773-776 (2000).
2. B. Shan, and Z. Chang, "Dramatic extension of the high-order harmonic cutoff by using a long-wavelength driving field", *Phys. Rev. A* 65, 011804 (2001).
3. B. Shan, A. Cavalieri, and Z. Chang, "Tunable high harmonic generation with an optical parametric amplifier", *Appl. Phys. B* 74, S23-S26 (2002).
4. T. Brabec, and F. Krausz, "Intense few-cycle laser fields: frontiers of nonlinear optics", *Rev. Mod. Phys.* 72, 545 (2000).
5. J. C. Solem, and G. C. Baldwin, "Microholography of living organisms", *Science* 218, 229 (1982).
6. M. Howells, C. Jacobsen, J. Kirz, R. Feder, K. McQuaid, and S. Rothman, "X-ray holograms at improved resolution: a study of zymogen granules", *Science* 238, 514 (1987).
7. J. E. Trebes, S. B. Brown, E. M. Campbell, D. L. Matthews, D. G. Nilson, G. F. Stone, and D. A. Whelan, "Demonstration of x-ray holography with an x-ray laser", *Science* 238, 517 (1987).

8. Ph. Zeitoun, G. Faivre, S. Sebban, T. Mocek, A. Hallou, M. Fajardo, D. Aubert, Ph. Balcou, F. Burgy, D. Douillet, S. Kazamias, G. de Lachèze-Murel, T. Lefrou, S. le Pape, P. Mercère, H. Merdji, A. S. Morlens, J-P. Rousseau, and C. Valentin, "A high-intensity highly coherent soft x-ray femtosencond laser seeded by a high harmonic beam", *Nature* 431, 426 (2004).
9. J. Tate, T. Auguste, H. G. Muller, P. Salières, P. Agostini, and L. F. DiMauro, "Scaling of wave-packet dynamics in an intense midinfrared field", *Phys. Rev. Lett.* 98, 013901 (2007).
10. P. B. Corkum, "Plasma perspective on strong-field multiphoton ionization", *Phys. Rev. Lett.* 71(13), 1994-1997 (1993).
11. M. Lein, N. Hay, R. Velotta, and P. L. Knight, "Role of the intramolecular phase in high-harmonic generation", *Phys. Rev. Lett.* 88 (18), 183903 (2002).
12. T. Kanai, S. Minemoto, and H. Sakai, "Quantum interference during high-order harmonic generation from aligned molecules", *Nature* 435, 470-474 (2005).
13. C. Vozzi, F. Calegari, E. Benedetti, J-P Caumes, G. Sansone, S. Stagira, M. Nisoli, R. Torres, E. Heesel, N. Kajumba, J. P. Marangos, C. Altucci, and R. Velotta, "Controlling two-center interference in molecular high harmonic generation", Phys, Rev. Lett. 95, 153902 (2005).
14. R. Torres, N. Kajumba, J. G. Underwood, J. S. Robinson, S. Baker, J. W. G. Tisch, R. de Nalda, W. A. Bryan, R. Velotta, C. Altucci, I. C. E. Turcu, and J. P. Marangos, "Probing molecular structure of polyatomic molecules by high-order harmonic generation", *Phys. Rev. Lett.* 98, 203007 (2007).
15. J. Itatani, J. Levesque, D. Zeidler, H. Niikura, H. Pépin, J-C Kieffer, P. B. Corkum, and D. M. Villeneuve, "Tomographic imaging of molecular orbitals", *Nature* 432, 867-871 (2004).
16. S. Patchkovskii, Z. Zhao, T. Brabec, and D. M. Villeneuve, "High harmonic generation and molecular orbital tomography in multielectron systems: beyond the single active electron approximation", *Phys. Rev. Lett.* 97, 123003 (2006).
17. S. Baker, J. S. Robinson, C. A. Haworth, H. Teng, R. A. Smith, C. C. Chirila, M. Lein, J. W. G. Tisch, J. P. Marangos, "Probing proton dynamics in molecules on an attosecond time scale", *Science* 312, 424-427 (2006).
18. P. W. Dooley, I. V. Litvinyuk, Kevin F. Lee, D. M. Rayner, M. Spanner, D. M. Villeneuve, and P. B. Corkum, "Direct imaging of rotational wave-packet dynamics of diatomic molecules", *Phys. Rev. A* 68, 023406 (2003).
19. K. Burnett, V. C. Reed, J. Cooper, and P. L. Knight, "Calculation of the background emitted during high-harmonic generation", *Phys. Rev. A* 45, 3347-3349 (1992).
20. J. Itatani, D. Zeidler, J. Levesque, M. Spanner, D. M. Villeneuve, and P. B. Corkum, "Controlling high harmonic generation with molecular wave packets", *Phys. Rev. Lett.* 94, 123902 (2005).